J. Mater. Environ. Sci. 7 (7) (2016) 2513-2525 *Elhousni et al.*
ISSN : 2028-2508
CODEN: JMESC

Study of sodium gluconate and cetyltrimethyl ammonium bromide as inhibitor for copper in Moroccan industrial cooling water systems

L. Elhousni[1], M. Galai[1], F.Z. ElKamraoui[2], N. Dkhireche[1], M. Ebn Touhami[1], R. Touir[1,3*], D. Chebabe[1], M. Sfaira[4], A. Zarrouk[5]

[1] *Laboratoire d'Ingénierie des Matériaux et d'Environnement : Modélisation et Application, Faculté des Sciences, Université Ibn Tofail, BP 133, Kénitra 14 000, Morocco.*
[2]*Laboratoire physico-chimique des matériaux et nano-matériaux, Faculté des sciences de Rabat Agdal, Université Mohamed V , Rabat, Morocco*
[3] *Centre Régional des Métiers de l'Education et de la Formation (CRMEF), Avenue Allal Al Fassi, Madinat Al Irfane BP 6210 Rabat, Morocco.*
[4]*Laboratoire d'Ingénierie des Matériaux, de Modélisation et d'Environnement, LIMME, Faculté des Sciences Dhar El Mahraz, Université Sidi Mohammed Ben Abdellah, USMBA, BP 1796 – 30000, Atlas – Fès, Morocco.*
[5] *LC2AME-URAC 18, Faculté des Sciences, Université Mohammed Premier, Oujda, Morocco*

Received 06 Apr 2016, Revised 08 May 2016, Accepted 12 May 2016
**Corresponding author. E-mail: touir8@yahoo.fr & touir8@gmail.com (R. Touir); Phone: +212670526959*

Abstract
This work based on the study of corrosion, scale-forming and microorganism inhibition of copper in Moroccan cooling water system by Sodium gluconate (SG), Cetyltrimethyl ammonium bromide (CTAB) and their mixture using electrochemical measurements coupled to scanning electron microscopy (SEM). It is found that the SG inhibits cathodic reactions indicating that it is acted as a cathodic type inhibitor and its inhibition is about 95 % at 10^{-3} M. In addition, the results showed that the CTAB acts as a mixed-type inhibitor and the best inhibition is at 15 ppm. So, the synergistic effect between SG and CTAB was investigated. It is showed that the CTAB addition decreased the performance of the SG from 95 % to 88 % and the performance of the mixture increase with immersion time. However, the polarization curves showed that this mixture acts as mixed-type inhibitor. The potential of zero charge (PZC) of copper was determined by AC impedance, and the mechanism of adsorption was discussed. Finally, the SEM observations confirmed that the mixture was a corrosion, scale and microorganism inhibitor after one day of immersion.

Keywords: Corrosion inhibition; scaling and microorganism; Copper, cooling water systems; Formulation; SEM

1. Introduction
Water is the most commonly used cooling fluid to remove unwanted heat from heat transfer surfaces. At the present time, some of the demand for better utilization of the limited water supplies is due to population growth and increasing development. Due to this, open recirculating cooling water systems that reuse cooling water are frequently used at large central utility stations, at chemical, petrochemical, and petroleum refining plants, in steel and paper mills, and at all types of processing plants **[1]**. Open recirculating cooling water systems continuously reuse the water that passes through the heat transfer equipment. The only function performed by a cooling tower is to cool the warmed water. The cooling water circulates to operating units where it picks up heat while cooling or condensing process streams and the resulting warm water is returned to the cooling tower.
However, copper has been one of the preferred materials in industry such as cooling water systems due to its high electrical and thermal conductivities, mechanical workability, and its relatively noble properties. It is widely used in many applications in electronic industries, and communications as a conductor in electrical power lines, and pipelines for domestic and industrial water utilities, including sea water, heat conductors and heat exchangers **[2]**.

Thus, copper corrosion and its inhibition in a wide variety of media, particularly when they contain chloride ions, have attracted the attention of many investigators **[2-13]**. In addition, copper materials are susceptible to corrosion and fouling by microorganisms in water cooling systems. So, in closed circulating cooling systems, the copper corrosion is inevitable, but it can be restrained. The corrosion current is dependent on the conductivity, the dissolved O_2 and CO_2, the pH, the temperature, the water flow velocity and the difference of galvanic potential (dissimilar metallurgy).

However, the use of inorganic or organic compounds and their derivatives provide an effective protection to copper and its alloys in aggressive medium **[14-15]**. This protection is ascribed to the chelation action heterocyclic part of the chemical compound and the formation of barrier layer between the inhibitor and the metal surface preventing metal reaction and dissolution. The barrier layer is attributed either to the presence of vacant d orbitals in copper atom that form coordinative bonds with atoms donate electron such as nitrogen, sulfur, phosphorous, or to strong π- interaction between the aromatic rings through the nitrogen-containing heterocyclic part of the inhibitor **[16]**.

In the present work, the influence of sodium gluconate (SG), biocide (CTAB) and their mixture as corrosion, scale and microorganism inhibitors for copper in Moroccan industrial cooling water system was investigated by using electrochemical measurement and SEM observations. In addition, the mechanism action of the mixture was also studied.

2. Experimental Procedure

A conventional three-electrode cell was utilized with a large area Pt counter and Ag/AgCl reference electrodes. The chemical composition of copper, which used such as working electrode, is summarized in Table 1. The rod was mounted into glass tube of appropriate internal diameter by epoxy resin leaving a front surface area of 1 cm^2 to contact the test solution. Before each experiment, the surface electrode was abraded using emery paper at different grades (from 100 to 1200), cleaned with acetone, washed with distilled water, and dried at hot air. All potentials were measured and referred to the Ag/AgCl reference electrode. The cooling water solution was used from industry MAC/Z and its composition is displayed in Table 2. This composition represents the average amount of various ions present in the waters used in cooling waters system. According to the literature **[17, 18]**, this solution was corrosive and scale-forming. The temperature of the solution is 32 ± 1 °C. The electrolyte was in contact with air without any purging of dissolved oxygen.

All Electrochemical experiments were performed using Potentiostat/Galvanostat PGZ 100 monitored by a personal computer and Voltalab.4.0.

The sodium gluconate (SG) (M = 218.1371 ± 0.0077 g/mol, Melting Point = 175 °C, soluble in water) where its structure is presented in Figure 1a, was used as a corrosion inhibitor. The SG is a sequestering agent of the first order because it combines excellent chelating properties and stability, especially under extreme conditions (high alkalinity, high temperatures), to the remarkable features of biodegradability. It is also systematically used in many industries such as: concrete and mortar admixtures, industrial detergency, degreasing metal surfaces **[19]** and other applications published and patented throughout our laboratory **[20-21]**.

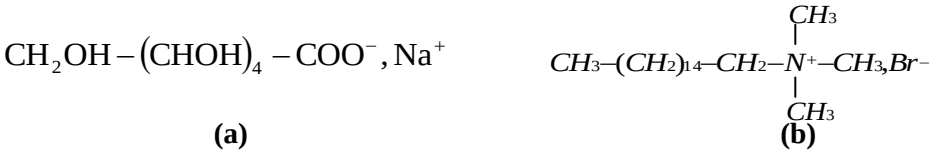

Figure 1: Chemical formula of the (a) sodium gluconate (SG) and (b) cetyltrimethylammonium bromid (CTAB)

The cetyltrimethylammonium bromide ($C_{19}H_{42}BrN$), is a commercial product, courteously purchased from FLUKA Company (Denmark), its purity is 96 % and was used as corrosion and biofilm inhibitor. It was evaluated using the minimal inhibitory concentration (MIC) techniques **[22,23]**. The chemical structure of this compound is presented in Figure 1b, as biocide, whose goal is the reduction of the microbial load present at the cooling circuits.

The potentiodynamic polarization experiments were undertaken using a scan rate of 1 mV s^{-1} to achieve quasi-stationary conditions. The obtained polarization curves were corrected for ohmic drop with the electrolyte resistance determined by electrochemical impedance spectroscopy. The current density values were determined using the following equation [**24**] :

$$i = i_a + i_b = i_{corr}\{\exp[b_a \times (E - E_{corr})] - \exp[b_c \times (E - E_{corr})]\} \quad (1)$$

where i_{corr} is the corrosion current density (A cm^{-2}), b_a and b_c (V^{-1}), (V^{-1}), are the Tafel constant of anodic and cathodic reactions, respectively. These constant are linked to the Tafel slope β (V/dec) in usual logarithmic scale by:

$$\beta = \frac{\ln(10)}{b} = \frac{2.303}{b} \quad (2)$$

The inhibition efficiency (η_{PP}) was calculated using the following equation:

$$\eta_{PP} = \frac{i_{corr}^0 - i_{corr}}{i_{corr}^0} \times 100 \quad (3)$$

where i_{corr}^0 and i_{corr} are the corrosion current density values without and with the inhibitor, respectively.
The impedance were recorded at the open circuit potential (OCP) in the frequency domain from 100 KHz down to 0.1 Hz using superimposed ac signal of 10 mV peak to peak. To achieve reproducibility, each experiment was carried out at least twice. The obtained impedance data were analyzed in term of equivalent electrical circuit using Z-view program. So, the inhibition efficiency was evaluated from R_p with the relationship:

$$\eta_{EIS} = \frac{R_p - R_p^o}{R_p} \times 100 \quad (4)$$

where, R_p^0 and R_p are the polarization resistance values in the absence and presence of inhibitor.
The morphology of the corrosion products formed on the surface of Cu in the industrial cooling water in the absence and presence of SG and CTAB were determined by SEM examinations using a Traktor TN-2000 energy dispersive spectrometer.

Table 1: Chemical composition of copper

Elements	Zn	Pb	P	Mn	Fe	Ni	Si	Mg
Wt.%	0.0031	0.0022	0.0008	<0.0004	0.0022	0.0054	<0.0005	0.0002
Elements	Cr	Te	As	Sb	Cd	Bi	Ag	Co
Wt.%	<0.0003	0.0073	<0.0002	<0.0005	<0.0002	<0.0005	0.0014	<0.0010
Elements	Al	S	Zr	Au	B	Ti	Se	Cu
Wt.%	< 0.0005	< 0.0002	<0.0003	< 0.0005	< 0.0004	< 0.0002	< 0.0002	99.976

Table 2: Chemical composition of the cooling water used in this research with the conductivity and the pH are respectively 1803 µS cm^{-1} and 8.2.

Elements	Cl^-	SO_4^{2-}	HCO_3^-	NO_3^-	PO_4^{3-}	F^-	Ca^{2+}	Mg^{2+}	Na^+	K^+	NH_4^+	NO_2^-
C (mg/L)	300	130	284	0.7	0.1	0.77	80	67	193	7	0.01	3.7

3. Results and discussion

3.1. Inhibitive effect of SG

The potentiodynamic polarization behavior of copper in industrial cooling water without and with SG is shown in Figure 2 at 305 K. Their electrochemical corrosion parameters are presented in Table 3.
Generally, in aerated aqueous solution, the cathodic reaction is either water and/or the oxygen reduction reaction according to **[25**, **26]** the following equations**:**

$$O_2 + 2H_2O + 4e^- \leftrightarrow 4\ HO^- \qquad E(O_2/HO^-) = -0.44\ V/Ag/AgCl \quad (5)$$

$$2\ H_2O + 2e^- \leftrightarrow H_2 + 2\ HO^- \qquad E(H_2O/H_2) = -1.2\ V/Ag/AgCl \quad (6)$$

This is because copper corrodes rapidly to form a compact and porous film of cuprous oxide and the oxide is in good electrical contact with the underlying metal **[3**, **27]** (Equation 7). However, the anodic reaction of copper can be represented in all solutions as follows **[3**, **28]** (Equation 7-10):

$$2Cu + H_2O \leftrightarrow Cu_2O + 2H^+ + 2e^- \quad (7)$$

$$Cu \leftrightarrow Cu^{+} + 1e^{-} \quad (8)$$

$$Cu^{+} + Cl^{-} \leftrightarrow CuCl \quad (9)$$

$$CuCl + Cl^{-} \leftrightarrow CuCl_2^{-} \quad (10)$$

It is noted, for the range from 10^{-5} M to 10^{-3} M, that the inhibitor addition decreases gradually the anodic and cathodic current densities with any change in the corrosion potential. In addition, it is noted for 10^{-5} M of SG, that the corrosion potential is shifted by 70 mV (which < 85mV). This result can classify the SG as mixed-type inhibitor [**29**]. Table 3 shows that the inhibitor addition has a beneficial effect even at low concentrations and its effectiveness increased with concentration to reach a maximum at 10^{-3} M. This suggests by the formation of soluble SG complex **[30**, **31]**.

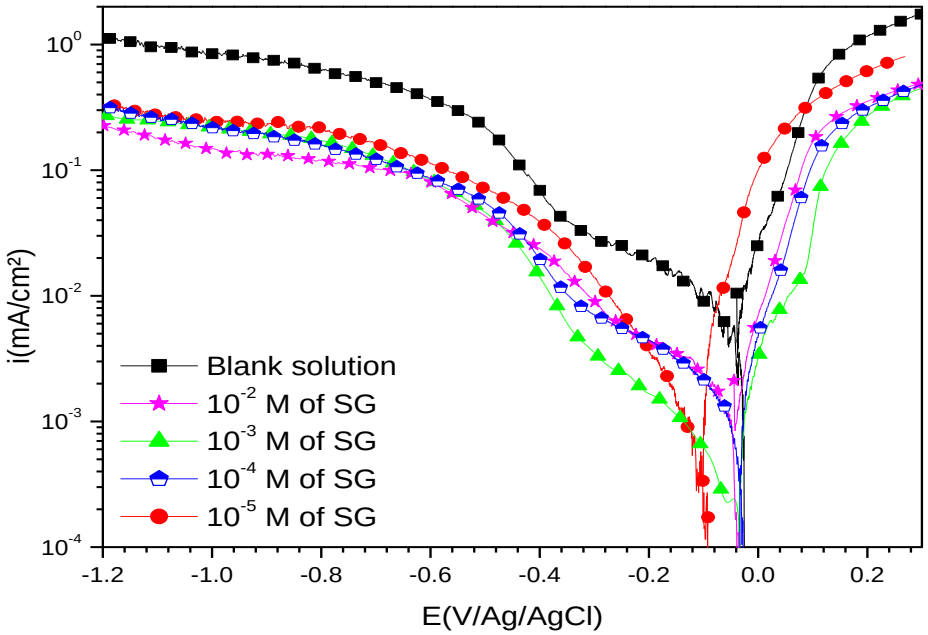

Figure 2: Potentiodynamic polarization curves for copper electrode in industrial cooling water at different concentrations of SG after 1 h of immersion at 305 K.

Table 3: Electrochemical parameters and inhibition efficiency for copper in industrial cooling water solution at different concentrations of SG.

Conc. of SG M	E_{corr} mV/Ag/AgCl	i_{corr} µA cm^{-2}	β_c mV/dec	β_a mV/dec	η_{PP} %
00	-24	8.44	-95	120	-
10^{-5}	-94	1.69	-166	77	79
10^{-4}	-29	0.78	-148	70	91
10^{-3}	-33	0.38	-150	104	95
10^{-2}	-35	0.90	-103	65	89

In order to confirm the performance of the SG, the electrochemical impedance spectroscopy was used in the same condition at the corrosion potential. The obtained results for copper after 1 h of immersion in corrosive solution without and with SG are presented in Figure 3. It may be noted that the obtained impedance responses were significantly changed by inhibitor addition. It is also noted that this plots consisted of two badly separated loops. The one at high frequency was attributed to the adsorbed species resistance due to adsorption of the molecules inhibitor and all other accumulated products. Conversely, the one at low frequency was usually attributed to the double layer capacitance and the charge transfer resistance. Because of this poor separation and in order to analyze the Nyquist plots impedance spectra more quantitatively, an equivalent electric circuit with two time constants was tried to reproduce these results by non linear regression calculation. This circuit for the impedance diagrams presented in Figure 3 is shown in Figure 4 and is similar to that for copper in neutral media **[32,33].**

However, it is worth pointing out that the application of an electrical circuit consisting of double layer capacitor does not always enable achieving satisfactory fitting to the experimental impedance data. The dispersion of the impedance data can be attributed to the surface heterogeneity, dislocations, impurities, grain boundaries, fractality, etc. In such case using an equivalent electrical circuit employing the double layer capacitance element is not a good enough approximation. The Constant Phase Element (CPE) was suggested instead of Cdl. So the impedance of the CPE can be described by the following equation:

$$Z_{CPE} = \left[Q(j\omega)^n\right]^{-1} \quad (11)$$

where j is the imaginary number, Q is the frequency independent real constant, $\omega=2\pi f$ is the angular frequency (rad s^{-1}), f is the frequency of the applied signal, n is the CPE exponent for whole number of n=1,0,−1, CPE is reduced to the classical lump element-capacitor (C), resistance (R) and inductance (L) [**34**]. The use of these parameters, similar to the constant phase element (CPE), allowed the depressed feature of Nyquist plot to be reproduced readily.

However, the effective calculated double layer capacitance (C) derived from the CPE parameters according to the following equation [**35**]:

$$C = Q^{\frac{1}{n}} \times R^{\frac{1-n}{n}} \quad (12)$$

The most important data obtained from the equivalent circuit are presented in Table 4. It may be remarked that R_p value increases with SG concentration with a maximum at 10^{-3} M. This change can result from a decrease in local dielectric constant and/or an increase in the thickness of the electrical double layer suggests that the inhibitors molecules function by adsorption at the metal–solution interface [**36, 37**]. EIS impedance study also confirms the inhibition character of inhibitor obtained with polarization curves measurements.

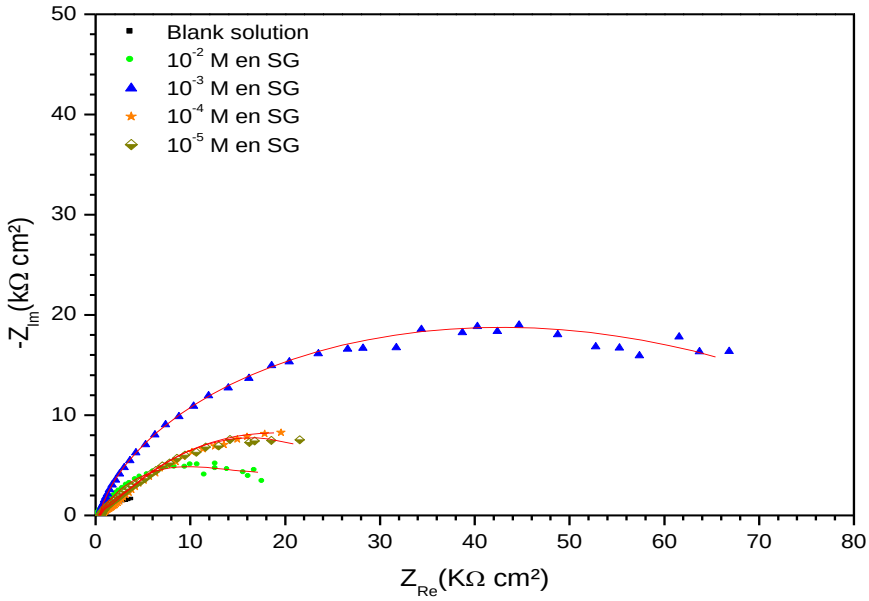

Figure 3: Nyquist diagrams for copper in industrial cooling water at different concentrations of SG obtained at E_{corr}.

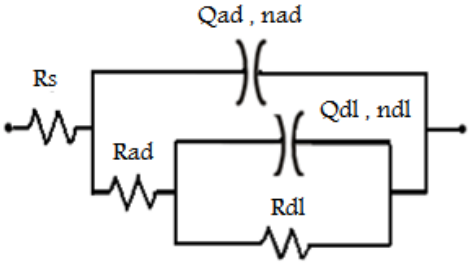

Figure 4: Electrical equivalent circuit proposed to simulate the impedance diagrams.

Table 4: Electrochemical impedance parameters and inhibition efficiencies for copper in industrial cooling water solution at different concentrations of SG.

Conc. of SG M	R_s Ω cm²	C_{ad} µF cm^{-2}	R_{ad} KΩ cm²	C_{dl} µF cm^{-2}	R_{ct} KΩ cm²	R_p KΩ cm²	η_{EIS} %
00	123	50	1	140	7.2	8	-
10^{-5}	523	38	5	96	24.2	28.67	72
10^{-4}	468	10	1.1	113	35	35.63	77
10^{-3}	459	5	4.7	18	92.7	101.14	92
10^{-2}	339	58	4.4	3.8	21.8	25.86	69

3.2. Inhibitive effect of CTAB

The potentiodynamic polarization behaviour of copper in industrial cooling water without and with different concentration of CTAB is showed in Figure 5 at 305 K. Their electrochemical parameters are presented in Table 5. In addition we have chosen this range of concentration according to the literature [**38**]. We have found that the corrosion rate in the presence of CTAB was smaller than that in its absence. In addition, it is noted that the CTAB addition decreases the cathodic and anodic current densities without change in the corrosion potential which it can be classified as a mixed-type inhibitor. It can be also seen that the i_{corr} values decreased with CTAB concentrations to reach a least value at 15 ppm. However, it is remarked that the anodic and cathodic Tafel slopes (b_a and b_c) change with the presence of CTAB indicating a change in the copper dissolution and dissolved oxygen reduction reactions.

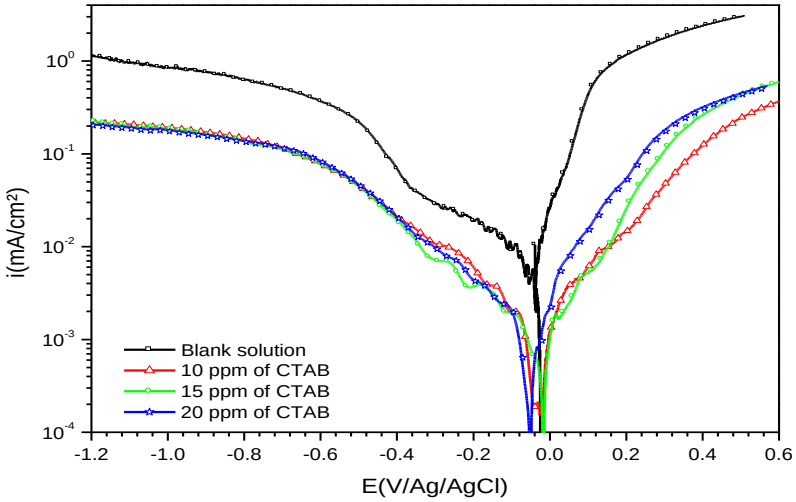

Figure 5: Potentiodynamic polarization curves for copper in industrial cooling water at different concentrations of CTAB after 1 h of immersion at 305 K.

Table 5: Electrochemical parameters and inhibition efficiencies for copper in industrial cooling water solution at different concentrations of CTAB.

Conc. of CTAB ppm	E_{corr} mV/Ag/AgCl	i_{corr} µA cm^{-2}	β_c mV/dec	β_a mV/dec	η_{PP} %
00	-24	8.44	-95	120	-
10	-16	1.85	-215	126	78
15	-16.2	1.1	-165	171	86
20	-48	1.4	-135	146	83

In order to confirm the performance of the CTAB such as mentioned above, the electrochemical impedance spectroscopy was used in the same condition at the corrosion potential. Figure 6 presented the obtained results. It is noted also that these diagrams were composed of two loops such as obtained in the case of SG. The similar findings were reported by other researchers, when they studied the effect of CTAB on low carbon steel in simulated cooling water system **[39-41]**. It is remarked, from the Table 6, that the polarization resistance R_p

increases gradually with CTAB concentration to reach a maximum at 15 ppm. This behaviour is the possible proof that biocide forms a protective layer on the copper surface. At 20 ppm, polarization resistance R_p decreases this can be explained by the development of oxide and/or hydroxide layer at the copper surface.

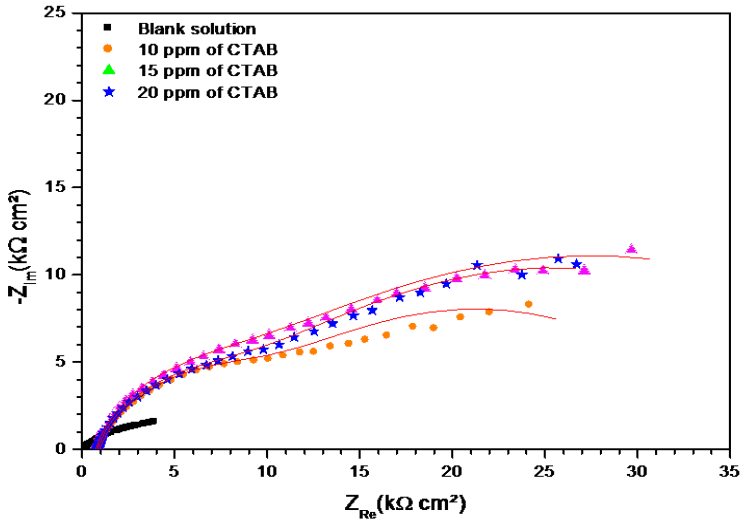

Figure 6: Nyquist diagrams for copper in industrial cooling water at different concentrations of CTAB at E_{corr}

Table 6: Electrochemical impedance parameters and inhibition efficiencies for copper in industrial cooling water solution at different concentrations of CTAB.

Conc. ppm	R_s Ω cm²	C_{ad} µF cm^{-2}	R_{ad} KΩ cm²	C_{dl} µF cm^{-2}	R_{ct} KΩ cm²	R_p KΩ cm²	η_{EIS} %
00	123	50	1	140	7.2	8	-
10	930	25	11.73	19	25	35.8	77.6
15	736	15	18.5	8.7	37.5	55.3	85.5
20	832	19	14.2	12	34.2	47.6	83

3.3. Effect of mixture (10^{-3} M SG + 15 ppm CTAB)

Figure 7 brings out the potentiodynamic polarization curves of copper in industrial cooling water without, and with 10^{-3} M of SG, 15 ppm of CTAB and their mixture. Their corresponding electrochemical parameters are listed in Table 7.

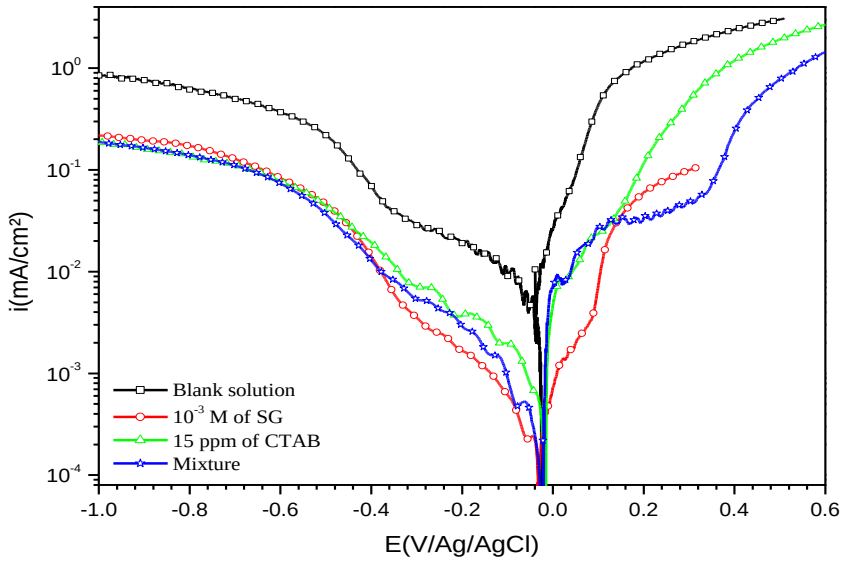

Figure 7: Potentiodynamic polarization curves for copper in industrial cooling water without and with 10^{-3} M of SG, 15 ppm of CTAB and their mixture after 1 h of immersion at 305 K.

Table 7: Electrochemical parameters and inhibition efficiencies for copper in industrial cooling water without and with 10^{-3} M of SG, 15 ppm of CTAB and their mixture.

	E_{corr} mV/Ag/AgCl	i_{corr} µA cm^{-2}	β_c mV/dec	β_a mV/dec	η_{PP} %
Blank solution	-24	8.44	-95	120	-
10^{-3} M of SG	-29	0.38	-150	104	95
15 ppm of CTAB	-16.2	1.1	-165	171	86
Mixture	-32	0.9	-144	133	89

It is clear that CTAB, SG and their mixture exhibit anodic and cathodic inhibition effect. It is noted also that the corrosion current density is more than sixteen five times lower in the presence of mixture when compared to the blank solution. In addition, it is found that the CTAB decrease slightly the performance of the SG where the inhibition efficiency decreases from 95 % to 89 %. In light of this information, CTAB exerts an antagonist effect. In addition, in the presence of mixtures, the anodic curve highlights a level of anodic current density over a wide potential range (240 mV). This result argues favor ably to the fact that these new formulations significantly enlarge the field of passive material. In fact, the inhibitor molecules passive ate the metal, acting as a barrier between the metal and corrosive medium. The corresponding current density of passivity is ca 31.2 µA cm^{-2}. This passivation enhances also the copper electrode resistance from pitting corrosion **[42]**.
However, Figure 8 shows the Nyquist diagrams for copper electrode in industrial cooling water without and with 10^{-3} M of SG, 15 ppm of CTAB and their mixture after 1 h of immersion at potential corrosion. Such as mentioned above, the obtained diagrams were composed of two loops, one at the high frequency and the second at the low frequency. The electrochemical data are extracted using the same electrical equivalent circuit presented in the Figure 4 and presented in Table 8. It is seen that the addition of CTAB to SG decreases slightly its effectiveness from 92 % to 87.7 %. Together, these findings show an antagonistic effect.

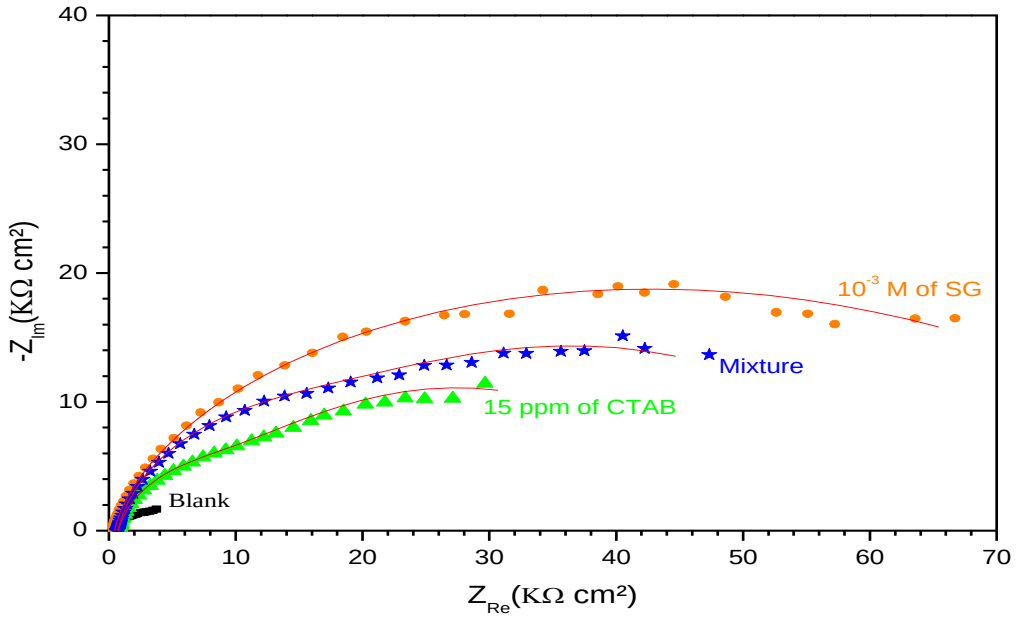

Figure 8: Nyquist diagrams for copper electrode in industrial cooling water without and with 10^{-3} M of SG, 15 ppm of CTAB and their mixture obtained at E_{corr}

Table 8: Electrochemical impedance parameters and inhibition efficiencies for copper in industrial cooling water without and with 10^{-3} M of SG, 15 ppm of CTAB and their mixture obtained at E_{corr}.

Compounds	R_s Ω cm²	C_{ad} µF cm^{-2}	R_{ad} KΩ cm²	C_{dl} µF cm^{-2}	R_{ct} KΩ cm²	R_p KΩ cm²	η_{EIS} %
Blank solution	123	50	1.0	140	7.2	8	-
10^{-3} M of SG	459	5	4.4	18	92.7	96.9	92
15 ppm of CTAB	736	15	18.5	8.7	37.5	55.3	85.5
Mixture	697	8	19	6.9	46.5	64.8	87.7

3.5. Effect of immersion time in the performance of mixture

The effect of immersion time on the formulation performance of copper in industrial cooling water is shown in Figure 9. The Nyquist plots consisted of two loops. The one at high frequency was attributed to the adsorbed film resistance due to adsorption of the inhibitors molecules and all other accumulated products. Conversely, the one at low frequency was usually attributed to the double layer capacitance and the charge transfer resistance. From longer immersion times, it was possible to characterize the layer surface modification by SEM analyses.
It is noted also that the impedance spectra reported in Figure 10 shows a decrease of the total impedance of the system with immersion time until 4 hours and became to increase beyond 6 hours. This increase suggests a strong inhibition of the dissolution processes occurring on the surface **[43, 44]**. The same equivalent circuit shown in Figure 4 was used to simulate the impedance spectra. The relevant simulated impedance parameters are shown in Table 9.

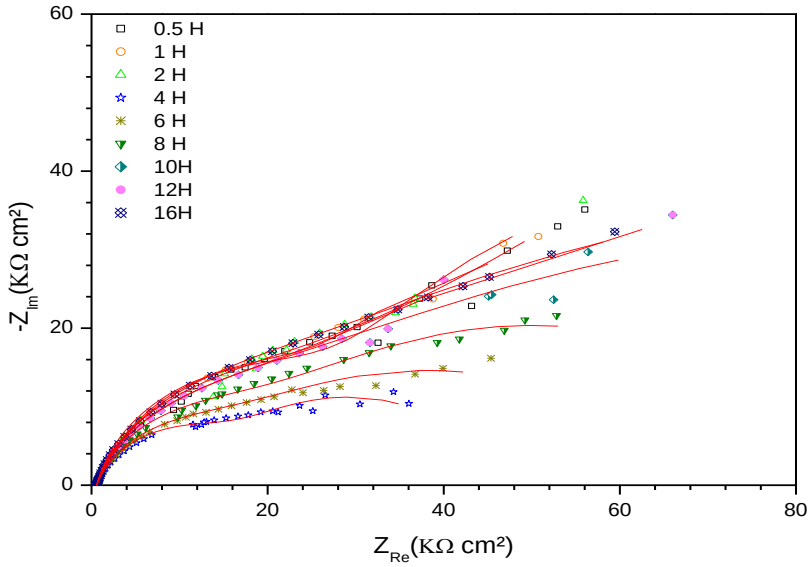

Figure 9: Nyquist diagrams for copper electrode in industrial cooling water with mixture obtained at different immersion time. Symbols: Experimental data, and Red lines: Fitting data.

Table 9: Electrochemical impedance parameters and inhibition efficiencies for copper in industrial cooling water with mixture at different immersion time.

Time h	R_s Ω cm²	C_{ad} µF/cm²	R_{ad} KΩ cm²	C_{dl} µF/cm²	R_{ct} KΩ cm²	R_p KΩ cm²	η_{EIS} %
0.5	587	12	22	49	106	127.41	93.7
1	579	14	40.4	101	45	84.82	90.6
2	588	11.5	35	89	42	76.4	89.5
4	603	20.7	18.8	196	26	44.20	81.9
6	597	17	18.6	96	47.4	65.40	87.7
8	588	15	23	85	63.3	85.71	90.7
10	585	13.8	22	49	71	92.42	91.3
12	585	13.5	25.4	56	81	105.82	92.4
24	584	12.8	26.8	46	99	125.22	93.6

It is noted that an increase of immersion time caused decrease and increase in C_{ad} and R_{ad} values, respectively, beyond 6 hours. A change in C_{ad} values might be explained in one of two ways based on Equation (13):

$$C_{ad} = \frac{\varepsilon_0 \times \varepsilon_r \times S}{d} \qquad (13)$$

where ε_0 is the vacuum permittivity, ε_r is the relative dielectric constant, S is the surface area of the investigated electrode and d is the thickness of the double layer.

Thus according to Equation (11) decrease in C_{ad} parameter can be caused by either decrease of the local dielectric constant or increase of the double layer thickness **[45]**. The former takes place when water molecules adsorbed on the copper surface are substituted by formulation molecules. The dielectric constant for water equals to 80. Once the greater area of the metal surface is covered with formulation molecules the C_{ad} values decrease. The increase of the double layer thickness is caused by formulation molecules.

3.6. Inhibition mechanism

Adsorption of some inhibitors on a corroding metal depends mainly on the charge of the metal surface, the charge or the dipole moment of surfactants, and the adsorption of other ionic species if it is electrostatic in nature **[46]**. The potential of zero charge (PZC) plays a very important role in the electrostatic adsorption process. So, the AC impedance study was used to evaluate the potential of zero charge (PZC) **[47, 48]**. A plot of C_{dl} values recorded for copper in industrial cooling water in the absence of inhibitors at each applied potential is shown in Figure 10. The obtained plot is a parabola with a minimum capacitance at about - 0.074 V/Ag/AgCl. This value can be called the PZC of copper in industrial cooling water, which is more negative than the corrosion potential (-0.024 V/Ag/AgCl). This means that the copper surface is positively charged at the corrosion potential.

For this finding of electrical charge of copper, we can postulate that the adsorption of SG and/or CTAB molecules can occur directly on the copper surface or compete with already adsorbed chloride and/or sulfide ions such as mentioned previously (Figure 11) **[41**,**49].**

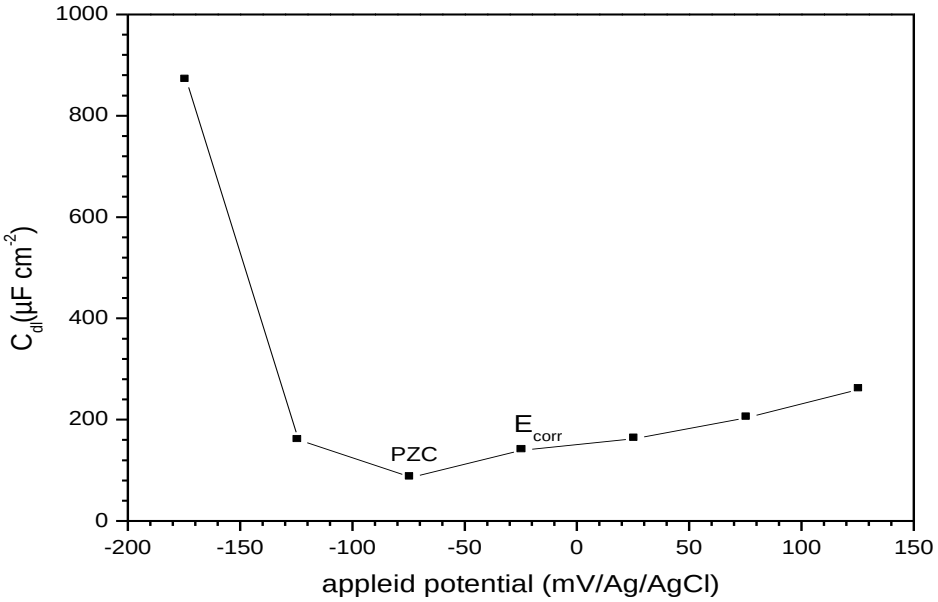

Figure 10: Relationship between C_{dl} values and the applied potential for a copper electrode in industrial cooling water solution.

However, the adsorption of these molecules can be described by two main types of interactions: physical adsorption or chemisorption. Generally, physical adsorption requires by the presence of both electrical charge of metal surface and charged species in solution while the chemisorption process involves charge sharing or charge-transfer from the molecules to the metal surface to form a coordinate type of bond. This is possible in case of a positive as well as a negative charge of the surface, the inhibitive action of CTAB can be result from physical (electrostatic) adsorption of the positively charge of nitrogen to the negatively charged copper surface, forming a barrier on the copper surface. In addition, the inhibitive action of SG can be also result from physical (electrostatic) adsorption of the negatively charge of oxygen to already adsorbed chloride and/or sulfide ions at the negatively charged copper surface.

Another possible mechanism therefore may be adsorption assisted by hydrogen bond formation between O and double liaison in biocide molecule and the oxidized surface (Cu_2O) species. So, the extent of adsorption by the respective modes depends on the metal surface nature. The adsorption layer acts as an additional barrier to the corrosive attack and enhances the performance of the passive layer as a result.

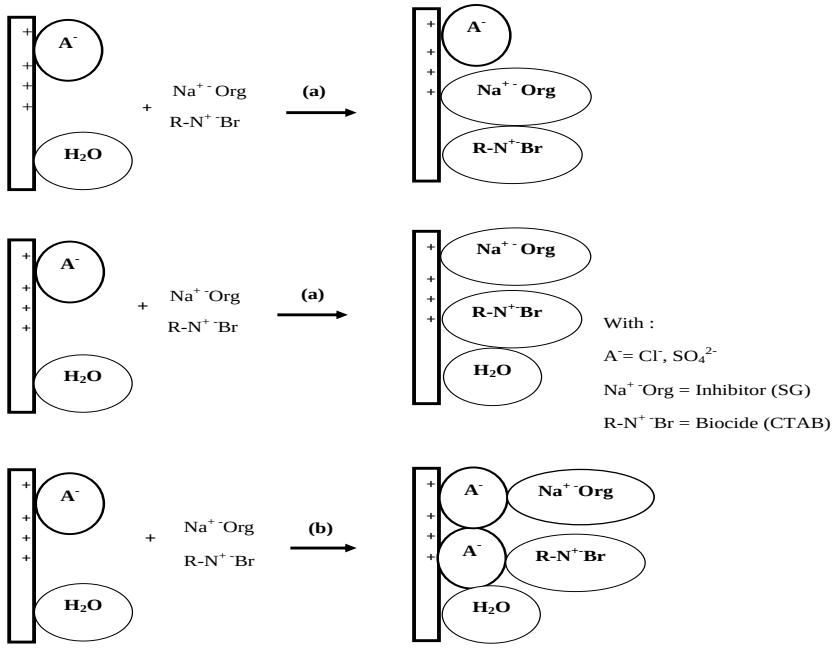

Figure 11: Mechanism of adsorption of SG and CTAB on the copper surface (a) competitive mode and (b) cooperative mode.

3.7. Scanning electron microscopy observations

Figure 12a shows the scanning electronic microscopy (SEM) micrographs of copper surface that have been exposed to the industrial cooling water solution for one day in the absence of mixture. It is shown the sample surface was greatly damaged during the immersion tests, as the corrosion products show a multi-layer morphology. The outer layer of the corrosion products appears uneven and rough, which is compactly adsorbed to the inner layer. In addition, it is remarked that these images show heterogeneous layer of scale-forming products.

In contrast, the metal surface immersed in industrial cooling water solution in the presence of mixture (Figure 12b) shows a large area free of corrosion, scale products and development of microorganisms and reveals the formation of an inhibitor layer. These results show that mixture acts as scale-forming, corrosion and microorganism inhibitor for copper and they are in accordance with the inhibition efficiency values obtained by electrochemical measurements.

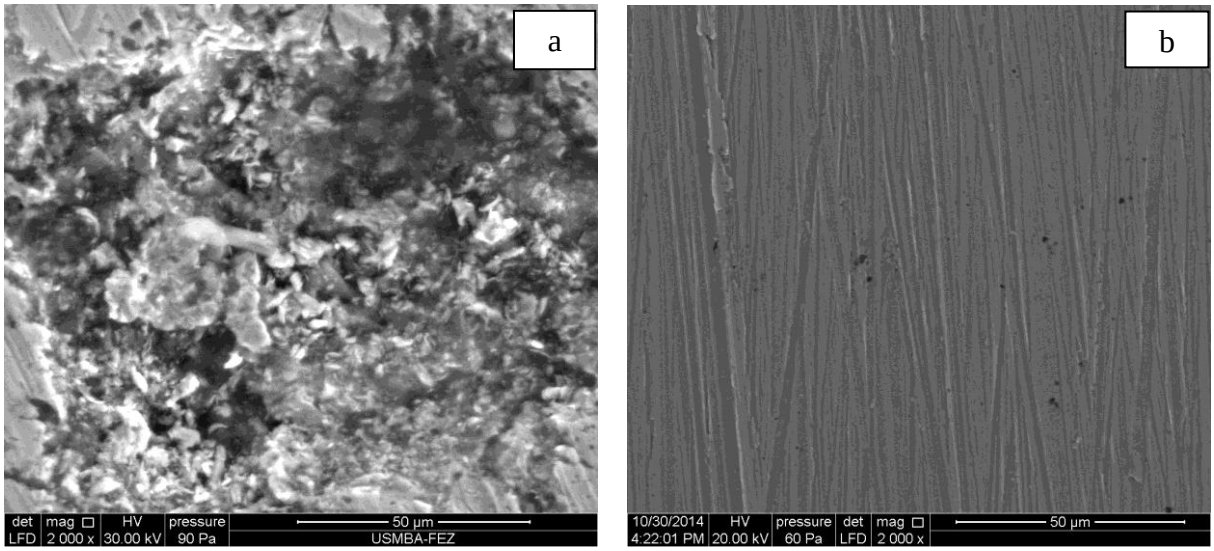

Figure 12: SEM pictures of copper electrode surface after one day of immersion in industrial cooling water solution: (a) the blank solution, (b) in the presence of mixture.

Conclusion

Electrochemical measurements coupled to SEM micrographs were used to investigate corrosion and scale inhibition of SG, CTAB and their mixture for copper in industrial cooling water system. It is found that the SG is a cathodic-type inhibitor and its performance reached 95% at 10^{-3} M of SG. In addition, the presence of CTAB at 15 ppm showed a better inhibition 88 % and is a mixed- type inhibitor. Such results were regarded as synergism effect between SG and CTAB to protect copper surface against corrosion and scale-forming. Additionally, EIS measurements, in agreement with potentiodynamic polarization data, proved the inhibitive properties of SG, CTAB and their mixture. It found also that the inhibition efficiency increased with immersion time beyond 6 h and reached 93.6 % at 24 h. The mechanism action of mixture showed that it can act by competitive and/or cooperative mode. The SEM micrographs showed a large area free of corrosion, scale-forming products and development of microorganisms in the presence of mixture and reveal the formation of an inhibitor layer.

References

1. Amjad Z., Butala D., J. Pugh, The influence of recirculating water impurities on the performance of calcium phosphate inhibiting polymers, in: Corrosion/99, NACE, Houston, 1999 (paper number 118).
2. Núńez L., Reguera E., Corvo F., Gonzalez E., and Vazquez C., *Corros. Sci.*, 47, (2005) 461.
3. El Warraky A., El Shayeb H. A., and Sherif E. M., *Anti-Corros. Methods Mater.*, 51, (2004) 52.
4. Bacarella L. and Griess J. C., *J. Electrochem. Soc*., 120, (1973) 459.
5. Lee H. P. and Nobe K., *J. Electrochem. Soc.*, 133, (1986) 2035.
6. Hoepner A. T. and Lattemann S., *Desalination*, 152, (2002) 133.
7. Adeloju S. B. and Daun Y. Y., *Br. Corros. J*., London, 29, (1994) 315.
8. Hamilton J. G., Farmer J. C., and Anderson R. J., *J. Electrochem. Soc*., 133, (1986) 739.
9. Al Hajji J. N. and Reda M. R., *Br. Corros. J*., London, 31, (1996) 125.
10. Breslin C. B. and Macdonald D. D., *Electrochim. Acta*, 44, (1998) 643.
11. Zumelzu E. and Cabezas C., *J. Mater. Process. Technol*., 57 (1996) 249.
12. Rocca E., Bertrand G., Rapin C., and Labrune J. C., *J. Electroanal. Chem*., 503, (2001) 133.
13. Christy A. G., Lowe A., Otieno-Alego V., Stoll M., and Webster R. D., J. *Appl.Electrochem*., 34, (2004) 225.
14. Soror T.Y., *The Open Corrosion Journal*. 45, (2009) 45-50.
15. Igual Muñoz A.I., García Antón J., Guiñón J.L., Pérez Herranz V., *Electrochim. Acta*, 50, (2004)957-966.
16. Popova I., Yates J.T. Jr. Adsorption and thermal behavior of benzotriazole chemisorbed on γ-Al_2O_3. Langmuir 13, (1997) 6169-6175.
17. Ramesh S., Rajeswari S., *Electrochim. Acta* 49 (2004) 811.
18. Saremi M., Dehghanian C., Mohammadi Sabet M., *Corros. Sci*. 48 (2006) 1404.
19. Roquette Frères 62080 Lestrem, France, site : www.roquette.fr/fr/Products/sodgluc.htm.
20. Larhzil H., Cissé M., Touir R., Ebn Touhami M., Cherkaoui M., *Electrochim. Acta* 53 (2007) 622-628.
21. The electroless bath and the Ni-P alloys coating process. French Patent N°FR2754831, date of publication 04/24/1998.
22. Choi D.J., You S.J., Kim J.G., *Mater. Sci. Engin. A* 335 (2002) 228-235.
23. Lancini G., Parenti F., Determination of the Minimal Inhibitory Concentration in Liquid, Springer, New York, 1988, p. 14.
24. Stern M., Geary A.L., *J. Electrochem. Soc*. 104 (1957) 56.
25. Otmacic H. and Stupnisek-Lisac E., *Electrochim. Acta* 48 (2002) 985.
26. Shaban A., Kálmán E., and Telegdi J., *Electrochim. Acta* 43 (1997) 159.
27. Ives D. J. and Rawson A. E., *J. Electrochem. Soc*. 109 (1962) 447.
28. Zhang D. Q.,. Gao L. X, and Zhou G.D., *J. Appl. Surf. Sci*. 225 (2004) 287.
29. El Faydy M., Galai M., El Assyry A., Tazouti A., Touir R., Lakhrissi B., Ebn Touhami M., Zarrouk A., *J. Mol. Liq.* 219 (2016) 396–404
30. Lahodny-Sarc O., Popov S., *Surf. Coat. Technol*. 34 (4) (1988) 537.
31. Roti J.S., Thomas P.A., in: Proceedings of the corrosion 84 NASE Conference, New Orleans, NASE, Houston, TX, 1984, p. 318.
32. Sfaira M., Srhiri A., Keddam M., Takenouti H., *Electrochim. Acta* 44 (1999) 4395.
33. Chen Y., Hong T., Gopal M., Jepson W.P., *Corros. Sci.* 42 (2000) 79.

34. Gerengi H., Darowicki K., Bereket G., Slepski P., *Corros. Sci.* 51(2009) 2573–2579.
35. Brug G.J., Van Den Eeden A.L.G., Sluyters-Rehbach M., Sluyters J.H., *J. Electroanal. Chem.* 176 (1984) 275–295.
36. Touir R., Dkhireche N., Ebn Touhami M., Sfaira M., Senhaji O., Robin J.J., Boutevin B., Cherkaoui M., *Mater. Chem. Phys*. 122 (2010) 1–9.
37. Lakhrissi L., Lakhrissi B., Touir R., Ebn Touhami M., Massoui M., Essassi E. M., *Arab. J. Chem. (*2014), http://dx.doi.org/10.1016/j.arabjc.2013.12.005.
38. El Bakri M., Touir R., Tazouti A., Dkhireche N., Ebn Touhami M., Rochdi A., Zarrouk A., *Arab. J. Sci. Eng.* 41 (2016) 75–88.
39. Belakhmima R.A., Dkhireche N., Touir R., Ebn Touhami M., *Mater. Chem. Phys*. 152(2015)85-94.
40. Rochdi A., Touir R., El Bakri M., Ebn Touhami M., Bakkali S., Mernari B., *J. Env. Chem. Eng*. 3 (2015) 233–242.
41. Touir R., Dkhireche N., Ebn Touhami M., El Bakri M., Rochdi A., Belakhmima R. A., *J. Saudi Chemical Society* 18 (2014) 873–881.
42. Wang X., Yang H., Wang F., *Corros. Sci.* 52 (2010) 1268–1276.
43. Jamil H.E., Shriri A., Boulif R., Bastos C., Montemor M.F., Ferreira M.G.S., *Electrochim. Acta* 44 (2004) 2753-2760.
44. Bommersbach P., Alemany-Dumont C., Millet J.P., Normand B., *Electrochim. Acta* 51 (2005) 1076–1084.
45. Gerengi H., Schaefer K., Ibrahim Sahin H., *J. Indus. Eng. Chem*. 18 (2012) 2204–2210.
46. Luo H., Guan Y.C. and Han K.N., *Corrosion* 54 (1998) 619.
47. Wu X., Ma H., Chen S., Xu Z. and Sui A., *J. Electrochem. Soc*., 146 (1999) 1847.
48. Damaskin B.B., Petrii O.A. and Batraktov B., Adsorption of Organic Compounds on Electrodes (Plenum Press, New York, 1971).
49. Touir R., Cenoui M., El Bakri M., Ebn Touhami M., *Corros. Sci.* 50 (2008) 1530–1537.